

Yaojun Du and N. A. W. Holzwarth: *Department of Physics, Wake Forest University, Winston-Salem, NC, USA*

Introduction

The thin film solid electrolyte LiPON developed at Oak Ridge National Laboratory,¹ has the composition of $\text{Li}_x\text{PO}_y\text{N}_z$, where $x = 2y + 3z - 5$, and is the most widely used solid electrolyte for thin film batteries and a number of other related technologies. In order to develop an understanding of the basic mechanisms of ionic conductivity in LiPON, we have performed atomistic modeling of idealized forms of synthetic and naturally occurring crystalline materials in the $\text{Li}_x\text{PO}_y\text{N}_z$ family. In previous work,² we focused on materials based on Li_3PO_4 which are characterized by Li^+ ions diffusing near isolated PO_4^{-3} groups. In these materials we computed vacancy and interstitial mechanisms of Li ion migration with energy barriers of 0.3-0.6 eV. In the present work, we consider natural and synthetic structures based on LiPO_3 which are characterized by Li^+ ions diffusing near infinitely long chains of PO_4 tetrahedra, connected by P-O-P bridging bonds. We also consider the effects of introducing N atoms into these materials, finding that N preferentially replaces O at the bridging sites to form P-N-P bridging bonds. We investigated the Li ion migration along and perpendicular to the chain directions.

Calculational Methods

We used the same methods as reported in our previous work.² The calculations were based on density functional theory³ using the local density approximation for the exchange-correlation functional.⁴ The calculations of electronic ground states and optimized structures were carried out using QUANTUM ESPRESSO (PWSCF) package⁵ with the ultrasoft pseudopotential formalism⁶ and also the PWPAAW code⁷ with the projector augmented wave formalism.⁸ Visualizations of the structures were obtained using XCrySDen and OpenDX software.⁹ Estimates of the migration energies E_m for Li ion diffusion were calculated using the nudged elastic band (NEB) method¹⁰ as implemented in the PWSCF code.

Survey of LiPON Family of Materials

The family of materials described by the stoichiometry of $\text{Li}_x\text{PO}_y\text{N}_z$ (with $x = 2y + 3z - 5$) includes a variety of crystal structures and material properties, which are related to the properties of LiPON electrolytes.

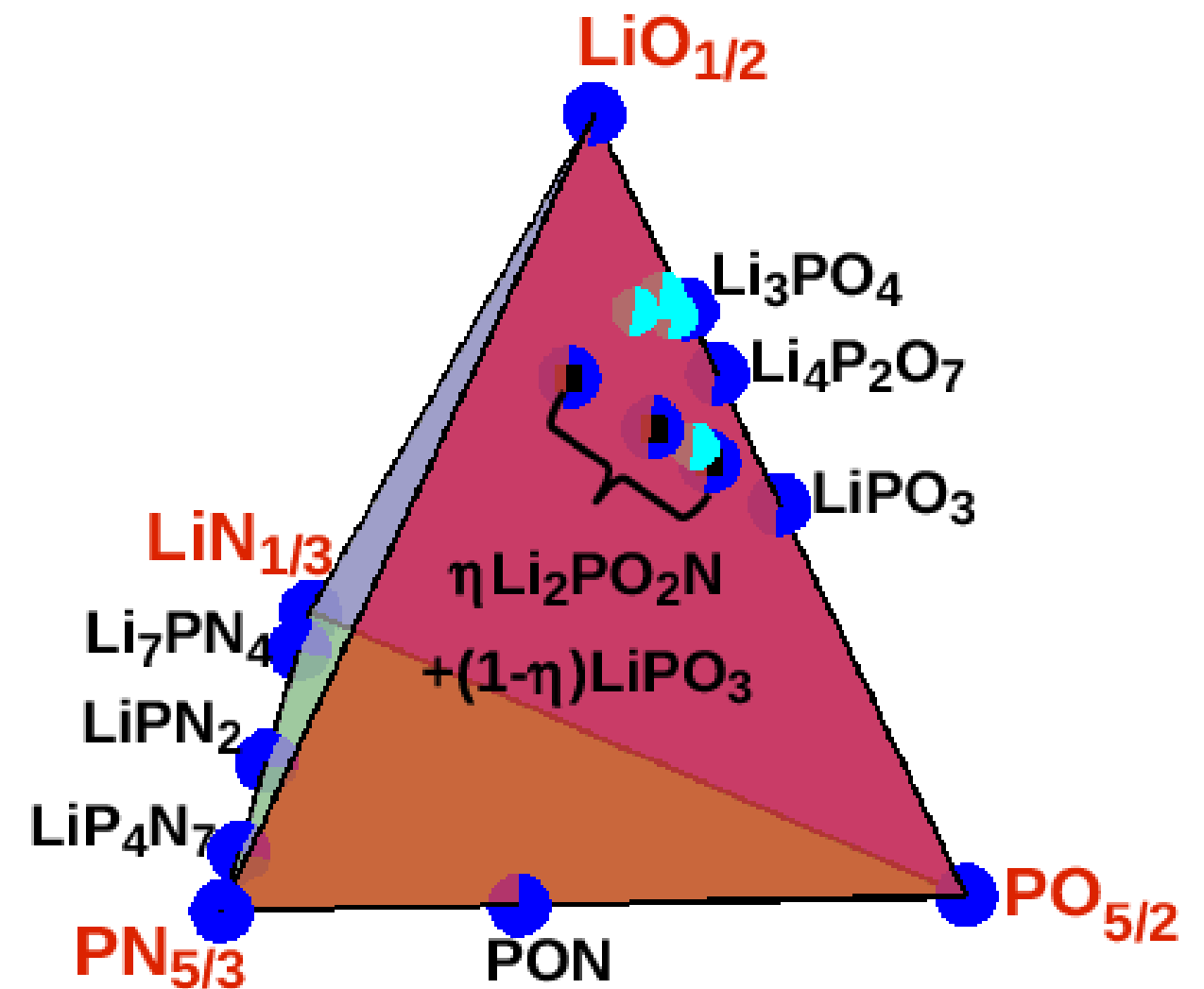


FIG.1 Composition diagram showing natural and synthetic crystalline materials (dark blue circles) based on $\text{LiO}_{1/2}$, $\text{LiN}_{1/3}$, $\text{PO}_{5/2}$, and $\text{PN}_{5/3}$ starting materials. The light blue circles indicate compositions of LiPON materials reported in the literature. The black squares indicate stable idealized phosphate chain structures having the composition of $\eta\text{Li}_2\text{PO}_2\text{N} + (1-\eta)\text{LiPO}_3$ studied in this work.

Formation energies of materials related to LiPON

Enthalpies of formation of materials can be used to determine relative equilibrium stabilities of the materials and to predict possible reactions between them. In computing total electronic energies of materials within density functional theory, we have access to enthalpies of formation at zero temperature, but systematic “correlation” errors limit the accuracy of the results. This is particularly a problem for estimating the total energies of molecular O₂ and N₂. In order to improve the formation energy estimates, we used the approach of Wang *et al.*,¹¹ and adjusted the total energies of both O₂ and N₂ by using a least squares fit to experimental standard formation energies of several N and O containing materials. Table I lists the calculated and experimental standard enthalpies of formation for materials related to LiPON. In addition to molecular O₂ and N₂ in their ground states, the reference states are solid Li in the bcc structure and white phosphorus (whose total energy was estimated from that of our calculated black phosphorus shifted by the experimental value of the relative energies between white and black phosphorus). All calculated values correspond to absolute zero temperature. The calculated results agree with the experimental results within 0.4 eV/FU. It is expected that relative energies between structurally and chemically similar materials is “considerable more accurate than the overall error.

A number of pure nitride materials (Li_xPN_z) have been studied experimentally¹² and we have calculated their formation energies. In general we find that the formation energies for the nitride materials, measured either per P or per Li, are considerably higher (less stable) than the corresponding oxides. Crystals of HP₄N₇ and NaP₄N₇ have been reported in the literature.¹³ Substituting Li into both of these structures, we computed two different stable structures for LiP₄N₇.

Among the most common pure oxide materials (Li_xPO_y), Li₃PO₄ which has an orthorhombic structure comprised of isolated PO₄ tetrahedra, has the lowest formation energy per P (most stable). LiPO₃ crystallizes in a structure with 100 atoms per unit cell¹⁴ comprised of chains of PO₄ connected by bridging bonds of P-O-P. In addition to studying this natural LiPO₃ material, we also found a stable LiPO₃ structure comprised of more regular PO₄ chains, with 20 atoms per unit cell and a formation energy 0.1 eV/P higher than that of the natural structure.

One of the interesting questions of the LiPON materials is the role of N. Our simulations show that it is energetically favorable for N to replace O at a bridging site compared with a tetrahedral O. By replacing all of the bridging O’s in our synthetic LiPO₃, we can form a stable nitrated chain structure with the stoichiometry of Li₂PO₂N. This material is found to have a formation energy of 0.7 eV/P higher than that of the synthetic LiPO₃. Partially nitrated chain structures were also considered. We found that for these synthetic structures, it is energetically more favorable for the bridging sites to alternate between O and N than to have pure -P-N-P- or -P-O-P- chains.

Standard Heats of Formation for Li_xPO_yN_z Materials

Formation energies for Li_xPO_yN_z and related materials. Energies are given eV per FU (formula unit), per P (phosphorus), and per Li (lithium). In addition to the references cited, data was obtained from the *CRC Handbook of Chemistry of Physics* and from the NIST website (<http://webbook.nist.gov/>). Values indicated with “*” were used in fit of O₂ and N₂ energies.

Material	Experiment	Calculation		
	$\Delta H/\text{FU}$	$\Delta H/\text{FU}$	$\Delta H/\text{P}$	$\Delta H/\text{Li}$
Li ₂ O ^a	-6.18 ± 0.03*	-6.13		-3.06
Li ₃ N ^b	-1.74 ± 0.03*	-1.58		-0.53
LiNO ₃	-5.01*	-5.40		-5.40
P ₂ O ₅ ^c	-15.46 ± 0.01*	-15.49	-7.74	
P ₂ O ₅ ^d	-15.76	-15.82	-7.91	
P ₃ N ₅	-3.32*	-3.23	-1.08	
PON ^e	-3.85 ± 0.05*	-4.04	-4.04	
Li ₇ PN ₄		-9.68	-9.68	-1.38
LiPN ₂		-3.70	-3.70	-3.70
LiP ₄ N ₇ ^f		-7.12	-1.78	-7.12
LiP ₄ N ₇ ^g		-7.19	-1.80	-7.19
Li ₃ PO ₄	-21.72*	-21.28	-21.28	-7.09
Li ₄ P ₂ O ₇		-34.09	-17.05	-8.52
LiPO ₃ ^h		-12.79	-12.79	-12.79
LiPO ₃ ⁱ		-12.72	-12.72	-12.72
Li ₂ PO ₂ N ⁱ			-12.07	-6.04
50-50 ^{i,j}			-12.43	-8.28
50-50 ^{i,k}			-12.23	-8.15
25-75 ^{i,l}			-12.53	-10.02
25-75 ^{i,m}			-12.41	-9.93

^aH. Kimura *et al.*, *J. Nucl. Mat.* **92**, 221 (1980). ^bH. Kimura *et al.*, *J. Nucl. Mat.* **91**, 200 (1980). ^c(hexagonal) W. S. Holmes, *Trans. Faraday Soc.* **58**, 1916 (1962). ^d(orthorhombic) Ref. [c] and Table 12.5 in N. N. Greenwood and A. Earnshaw *Chemistry of the Elements, Second Ed.*, Butterworth-Heinemann (1997) ^eF. Tessier *et al.*, *Chem. Mater.* **12**, 148 (2000) ^fDerived from NaP₄N₇ structure. ^gDerived from HP₄N₇ structure. ^hNaturally occurring crystal. ⁱSynthetic crystal. ^j50% Li₂PO₂N and 50% LiPO₃; alternating -P-N-P-O-P-N-P chains. ^k50% Li₂PO₂N and 50% LiPO₃; pure -P-N-P- and -P-O-P- chains. ^l25% Li₂PO₂N and 75% LiPO₃; alternating -P-N-P-O-P-N-P chains. ^m25% Li₂PO₂N and 75% LiPO₃; pure -P-N-P- and -P-O-P- chains.

Partial Densities of States of some LiPON materials

Partial densities of states (PDOS) of one-electron band structures can give qualitative insight into the bonding properties of the materials. The PDOS were calculated in the usual way:

$$N^a(E) \equiv \frac{2}{\sqrt{\pi}\Delta} \sum_{nk} f_{nk}^a W_{\mathbf{k}} e^{-(E-E_{nk})^2/\Delta^2}.$$

Here the factor of 2 is due to spin degeneracy, the factor $W_{\mathbf{k}}$ denotes the Brillouin zone weighting factor, and the smearing width parameter was chosen to be $\Delta = 0.1$ eV. For each state of band index n and wave vector \mathbf{k} , the factor f_{nk}^a denotes the charge within a sphere about atom a ; the radii were taken to be 1.6, 1.5, 1.4, and 1.4 bohr for Li, P, O, and N, respectively. The average partial densities of states $\langle N^a(E) \rangle$ were obtained by averaging the values over similar atomic spheres a . In Fig. 2 we distinguish between tetrahedrally bonded O sites (shaded blue curves) and bridging O sites (blue curve). Bridging N sites are indicated with a green curve; P and Li contributions are indicated with thick orange and thin black curves respectively. The energy range represents the $2p$ states of O and N with additional hybridization contributions from the $3s$ and $3p$ states of P and the $2s$ states of Li.

In Fig. 2, the bottom panel represents the density of states of crystalline Li_3PO_4 which contains only tetrahedral O sites, while the other panels represent materials having phosphate chains with both tetrahedral O sites and bridging O or N sites. In general, we find the states near the top of the valence band to be largely characterized by tetrahedral O $2p\pi$ states associated with PO_4 groups. Interestingly, the bridging O and N states have low energy contributions 4 or 5 eV below the bands dominated by tetrahedral O states. These low energy states are characterized by O or N $2p\sigma$ states which are lowered in energy because of the attractive fields of the 2 neighboring P ions in bridging site geometry. While the energy range of the PDOS contributions is similar in the natural and synthetic LiPO_3 , the distribution of states is much broader in the natural crystal compared with that of the synthetic crystal. This is undoubtedly due to the complexity of the natural crystal geometry compared with that of the synthetic structure. In the natural crystal structure, the phosphate chains are twisted about the chain axis with a periodicity of 5 phosphate groups, while in the synthetic structure the “twist” in the phosphate chain structure has a periodicity of only 2 phosphate groups. For the nitrated synthetic crystal $\text{Li}_2\text{PO}_2\text{N}$, one can see that the bridging N states are generally higher in energy than the corresponding bridging O states in the LiPO_3 structure. All of these materials are electronically insulating, although these density functional results are not expected to quantitatively estimate the band gaps that would be measured experimentally.

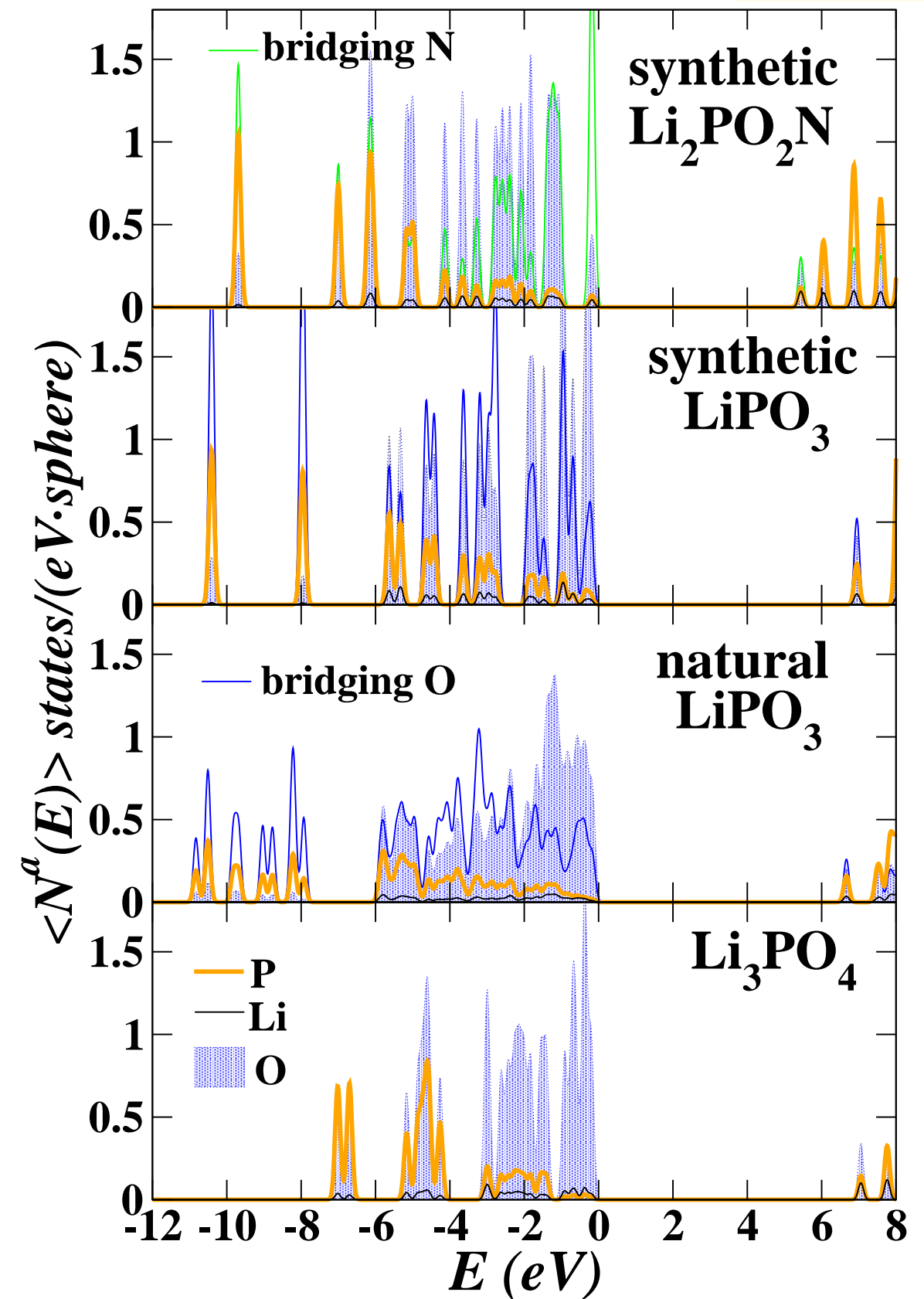


FIG. 2 Partial densities of states plots for several $\text{Li}_x\text{PO}_y\text{N}_z$ materials. The band energies (in eV) are plotted on the horizontal scale with the zero of energy set at the Fermi level.

Structural forms of PO₄ chain materials

LiPO₃ crystallizes into a monoclinic structure with 100 atoms per unit cell.¹⁴ The twisted PO₄ chains have a periodicity of 5 and are oriented along the $c - a$ direction as shown in Fig. 3. The majority of Li ions are located in channels between sets of four chains. The “majority” Li row is between 4 parallel rows of tetrahedral O’s from the PO₄ chains. There are two equivalent (but similar) sets of “majority” rows of Li in this structure. A small number of Li ions are sparsely distributed in “minority” rows in the crystal.

In addition to studying the natural LiPO₃, we also constructed more simple stable structures of synthetic LiPO₃. The structure shown in Fig. 4 has a twist periodicity in the PO₄ chains of 2 and an energy 0.1 eV/P higher than that of the natural structure. It has a similar distribution of phosphate bond lengths and angles and volume (20% larger). In this structure all of the Li ions are located in the “majority” rows. We also studied the effects of adding N to the synthetic structure. The fully nitrated bridge bond structure having a stoichiometry of Li₂PO₂N is shown in Fig. 5. In this case there are Li ions in the “minority” sites due to the presence of N. Fig. 6 shows a stable structure for a material having 50% synthetic Li₂PO₂N and 50% synthetic LiPO₃ with alternating N and O at the bridging sites.

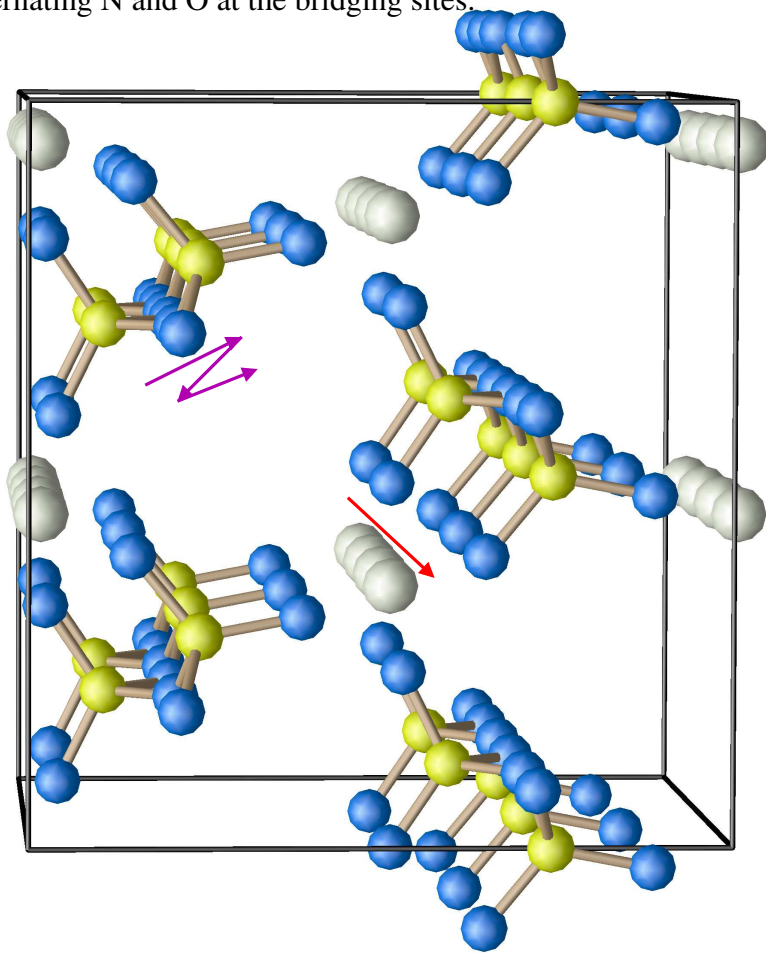


FIG. 4 Ball and stick model of synthetic LiPO₃ structure using same notation as in Fig. 3.

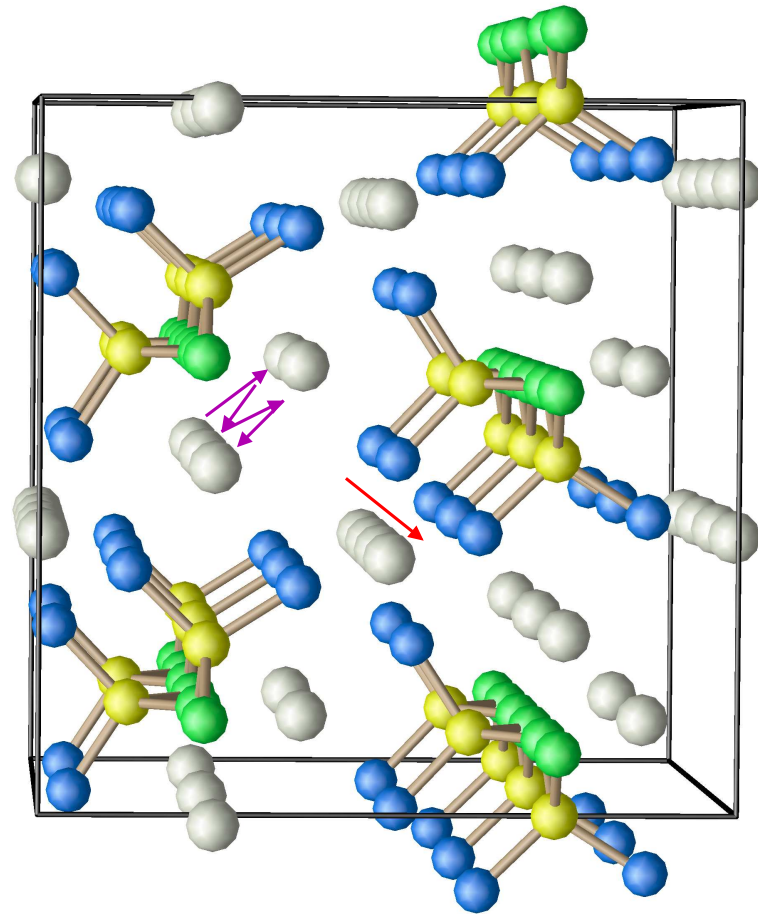


FIG. 5 Ball and stick model of synthetic Li₂PO₂N structure using same notation as in Fig. 3 with green balls denoting N sites.

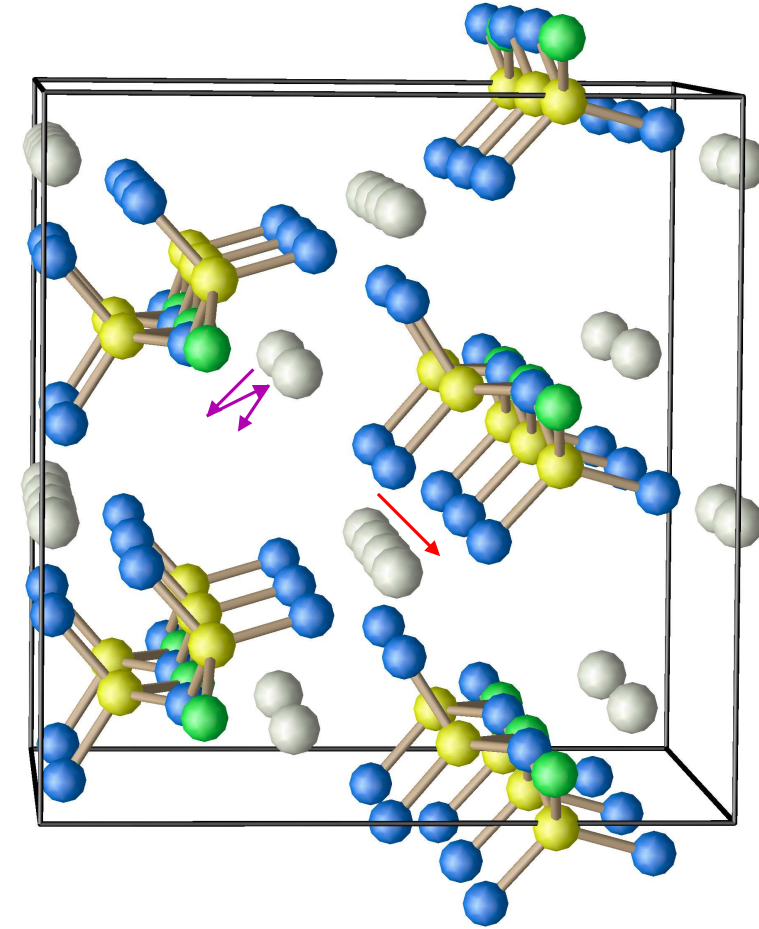


FIG. 6 Ball and stick model of synthetic 50% Li₂PO₂N and 50% LiPO₃ with alternating -P-O-P-N-P- chains using the same notation as Fig. 4.

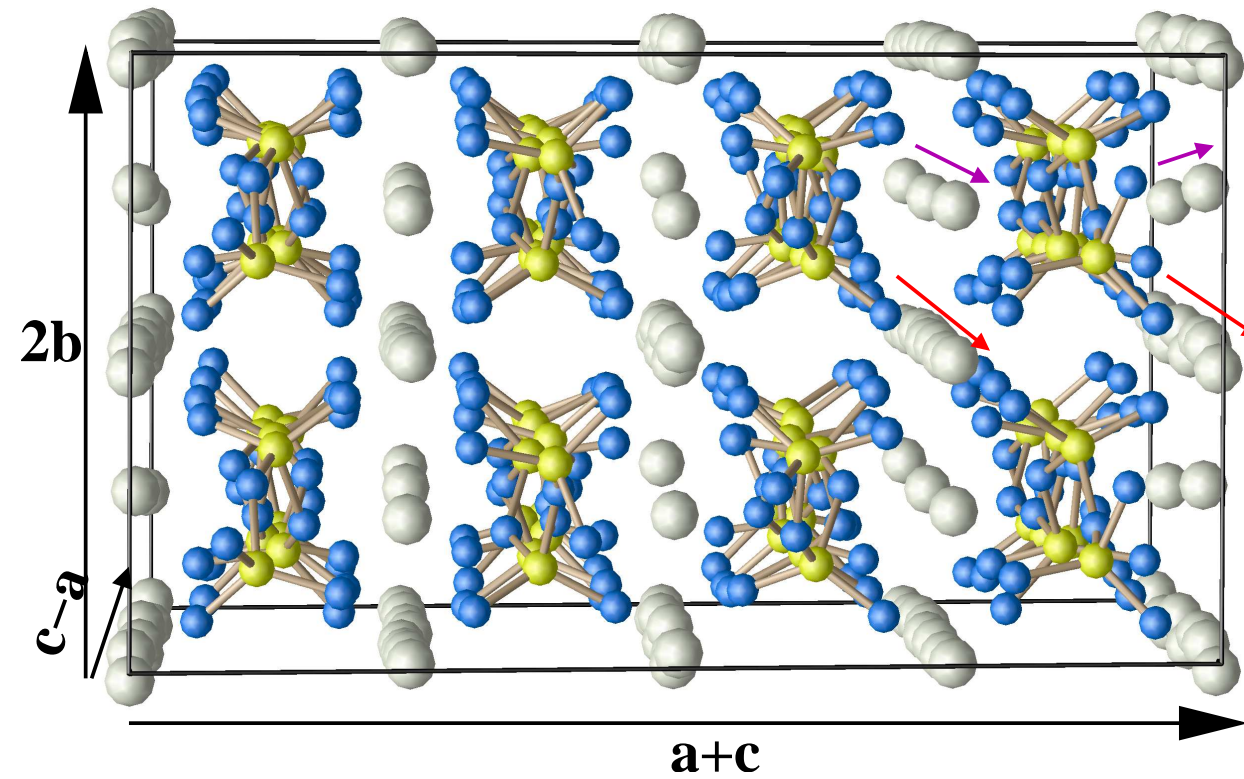


FIG. 3 Ball and stick model of natural LiPO₃ in its monoclinic structure using the same lattice conventions as defined in Ref. 14. Li, P, and O are shown with grey, yellow, and blue balls, respectively. Red arrows indicate Li ion vacancy migration paths in “majority” rows. Purple arrows indicate Li ion migration regions for “minority” sites.

Li ion migration energies in PO₄ chain materials

Using the NEB method¹⁰ we studied Li ion vacancy and interstitial migration energy barriers for natural and synthetic LiPO₃ and the synthetic nitrated materials. A summary of migration energy barriers is given below, followed by a detailed example for the case of Li ion vacancy migration in synthetic Li₂PO₂N.

Migration energy barriers, E_m (eV), calculated for Li ion migration paths along the chain directions in PO₄ chain materials. Preliminary results are indicated with (?).

Material	“Majority” row vacancy mechanism	“Minority” site vacancy mechanism	“Minority” site interstitial mechanism
natural LiPO ₃	0.6-0.8	2.0(?)	1.0 (?)
synthetic LiPO ₃	0.4	(none)	0.2
synthetic Li ₂ PO ₂ N	0.8	0.5	(none)
synthetic 50-50 material	(none)	(?)	0.4

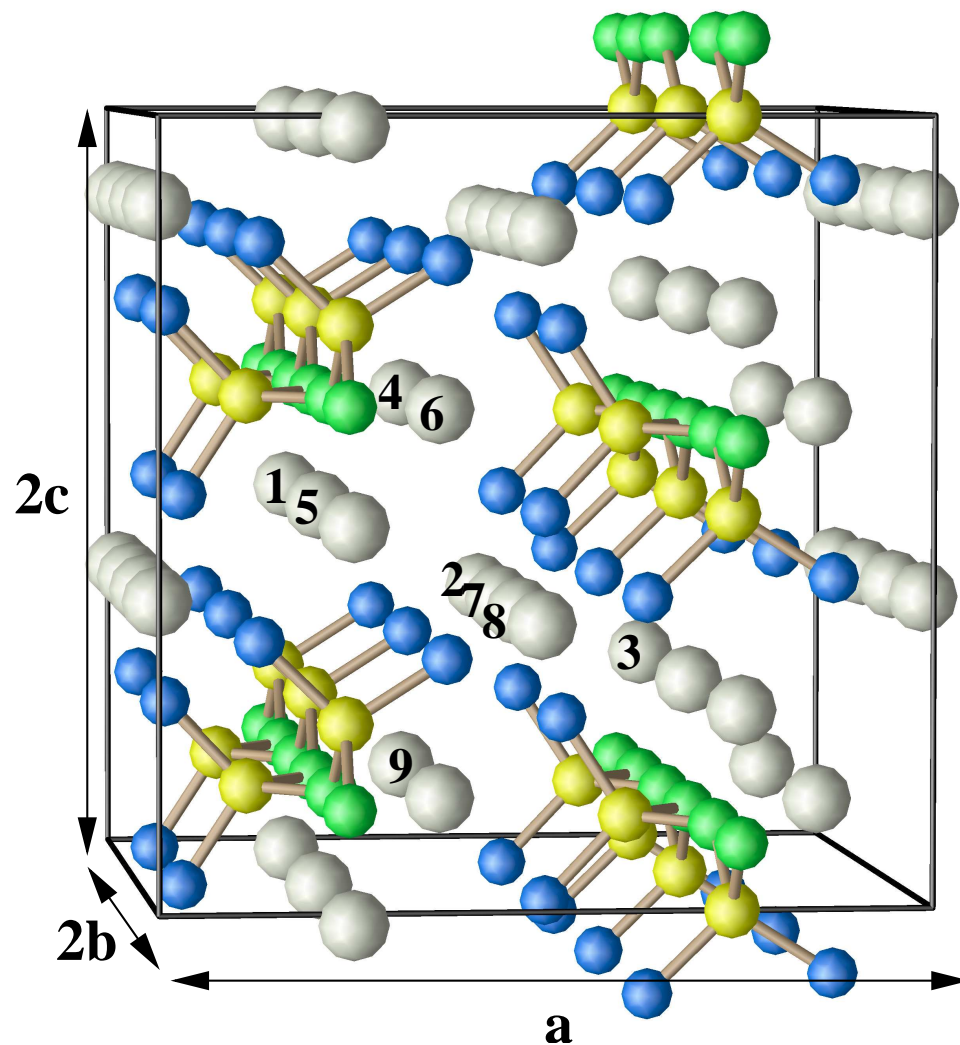


FIG. 7 Structure of synthetic Li₂PO₂N is shown with Li vacancy site labels used in migration energy analysis for paths along and perpendicular to the chain direction.

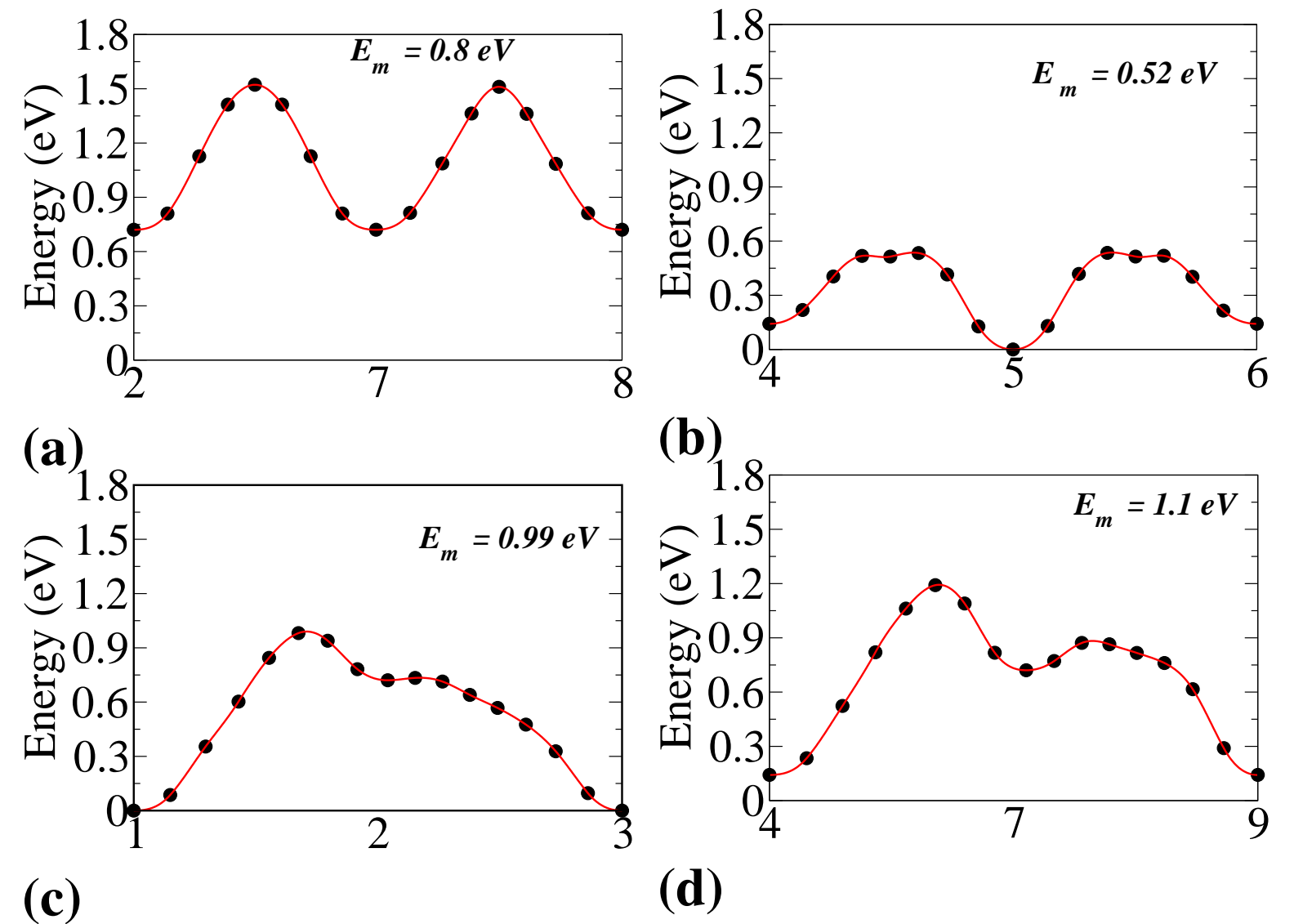


FIG. 8 An example of the detailed migration energy path analysis is shown in the four figures above, indicating energy paths of a migrating Li ion vacancy in synthetic Li₂PO₂N. Migration paths parallel to the P-N-P chain are shown in (a) for the “majority” row and (b) for the zig-zag “minority” sites, respectively. Migration paths perpendicular to the P-N-P chain are shown in (c) and (d) with much larger migration barriers than for the parallel paths. For migration paths along the chain directions, the “majority” row migration is characterized by 2.6 Å hops between adjacent vacancy sites in the chain direction. The “minority” site migration is characterized by 3.2 Å hops between adjacent vacancy sites in a zig-zag pattern with net motion along the chain direction. The zero of energy in these plots was taken at the lowest energy vacancy site which is located at a “minority” site. The corresponding lowest energy vacancy sites in a “majority” row is 0.7 eV higher.

Summary and Conclusions

We have made some progress towards our goal of developing a comprehensive picture of electrolyte properties of the $\text{Li}_x\text{PO}_y\text{N}_z$ family of materials, although much more work remains.

- A survey of the formation energies per phosphorus of known and constructed crystals shows that structures with isolated PO_4 groups have the lowest energy, followed by structures with isolated P_2O_7 dimers, followed by structures with infinite chains of PO_4 connected by bridging P-O-P bonds (LiPO_3). We also found that most of the phosphates have nitride analogs with higher formation energies. In addition to known crystal structures, we constructed new stable structures containing infinite phosphate chains. Our synthetic LiPO_3 has a formation energy of 0.1 eV higher than that of the natural structure. We also considered the effects of adding N to this structure, finding a stable $\text{Li}_2\text{PO}_2\text{N}$ structure with pure P-N-P bonds with a formation energy of 0.7 eV/P higher than that of the corresponding LiPO_3 structure. Thus, observed beneficial effects of N in LiPON materials is not simply reflected in the standard heat of formation results.
- We studied the Li ion migration in LiPO_3 in its natural and synthetic structures and also considered the effects of nitridation. In general, Li ion migration along the phosphate chain direction is energetically favored over migration perpendicular to the chains. For migration along the chain in the vacancy mechanism, Li ion migration in the “majority” row is 0.6-0.8 eV and 0.4 eV for the natural and synthetic structures, respectively. For the synthetic crystal, there are no “minority” Li sites, but interstitial Li ions introduced into the void region, diffuse with a very small (0.2 eV) energy barrier along the chain direction. When N (and the appropriate amount of Li) are introduced into the synthetic structure, the “minority” Li sites become occupied and these sites are energetically favored in the migration processes. For $\text{Li}_2\text{PO}_2\text{N}$, vacancy diffusion using the “minority” sites is energetically favored over the “majority” row sites. In fact, the most stable vacancy configuration in $\text{Li}_2\text{PO}_2\text{N}$ is located at a “minority” site. This is also true for mixed crystals of 50% $\text{Li}_2\text{PO}_2\text{N}$ and 50% LiPO_3 . For the natural crystal of LiPO_3 , the “minority” sites also include the most stable vacancy configuration, although we have not yet found those sites to contribute to the likely Li ion migration paths for either a vacancy mechanism or interstitial mechanism.
- We have obtained a lot of insight into Li ion diffusion processes by studying our synthetic structures. We have yet to establish the relationships of those structures to physically realizable electrolytes. On the other hand, there are some interesting similarities.
 1. The distribution of bond lengths and bond angles for the PO_4 groups are very similar for the two structures.
 2. In both structures, the majority Li row is surrounded by 4 parallel rows of tetrahedral O's from the neighboring chains. In the case of the natural structure, the 4 tetrahedral O rows come from 4 different PO_4 chains. For the synthetic structure, the 4 tetrahedral O rows come from 3 different PO_4 chains; two of the tetrahedral O rows are associated with a single chain.

Acknowledgements

This work was supported by NSF grant DMR-0705239. We would also like to thank G. Lopez for performing calculations on black phosphorus; R. Nofle, A. Lachgar, and R. Williams for helpful discussions; and G. Holzwarth and B. Kolb for matlab help.

Bibliography

- [1] N. J. Dudney, *Interface* **17**, 44 (2008).
- [2] Y. A. Du and N. A. W. Holzwarth, *Phys. Rev. B* **78**, 174301 (2008); Y. A. Du and N. A. W. Holzwarth, *Phys. Rev. B* **76**, 174302 (2007); Y. A. Du and N. A. W. Holzwarth, *J. Electrochem. Soc.* **155**, A999 (2007).
- [3] P. Hohenberg and W. Kohn. *Phys. Rev.* **136** B864, (1964); W. Kohn and L. J. Sham, *Phys. Rev.* **140** A1133, (1965).
- [4] J. P. Perdew and Y. Wang, *Phys. Rev. B* **45**, 13244 (1992).
- [5] Quantum-ESPRESSO is a community project for high-quality quantum-simulation software, based on density functional theory and coordinated by Paolo Giannozzi. <http://www.pwscf.org>.
- [6] D. Vanderbilt, *Phys. Rev. B* **41**, 7892 (1990)
- [7] N. A. W. Holzwarth, A. R. Tackett, and G. E. Matthews, *Comput. Phys. Commun.* **135**, 329,348 (2001).
- [8] P. E. Blöchl, *Phys. Rev. B* **50**, 17953 (1994); N. A. W. Holzwarth, G. E. Matthews, R. B. Dunning, A. R. Tackett, and Y. Zeng, *Phys. Rev. B* **55**, 2005 (1997).
- [9] A. Kokalj, *J. Mol. Graphics Modell.* **17**, 176 (1999); OPENDX – the open source software project based on IBM's Visualization Data Explorer. www.opendx.org.
- [10] H. Jónsson, G. Mills, and K. W. Jacobsen, in *Classical and Quantum Dynamics in Condensed Phase Simulations*. edited by B. J. Berne, G. Ciccotti, and D. F. Coker (World Scientific, 1998), pp 385-404.
- [11] L. Wang, T. Maxisch, and G. Ceder, *Phys. Rev. B* **73** 195107 (2006).
- [12] W. Schnick and J. Luecke, *Solid State Ionics* **38**, 271 (1990).
- [13] K. Landskron, E. Irran, and W. Schnick, *Chem. Eur. J* **5**, 2548 (1999); S. Horstmann, E. Irran, and W. Schnick, *Z. anorg. allg. Chem.* **624**, 221 (1998).
- [14] J. C. Guitel and I. Tordjman, *Acta Cryst.* **B32**, 2960 (1976); E. V. Murashova and N. N. Chudinova, *Crystall. Reports*, **46**, 942 (2001).